Two Simple Reinforced Concrete Beam Elements for Static and Dynamic Analysis

Deux éléments simples pour l'analyse statique et dynamique des structures porteuses en béton armé

Zwei einfache Balkenelement für die statische und dynamische Berechnung von Stahlbetontragwerken

M. ROSSI
Researche Associate
Swiss Federal Institute of Technology
Zurich, Switzerland

G. BAZZI
Research Associate
Swiss Federal Institute of Technology
Zurich, Switzerland

SUMMARY
Two simple beam elements for static and dynamic analysis of reinforced concrete members under bending, shear and normal forces are proposed. Basic assumptions are stated. The applicability is discussed making comparisons of computed and analytical or experimental results.

RÉSUMÉ
On presente deux éléments simples qui permettent le calcul statique et dynamique de structures porteuses en béton armé qui sont soumises à des sollicitations de flexion, d'effort tranchant et d'effort axial. On mentionne également les hypothèses qui sont à la base du calcul. Le champ d'application est illustré à l'aide de quelques exemples. On a fait une comparaison entre les résultats obtenus numériquement et ceux déterminés à l'aide d'essais ou de modèles analytiques.

ZUSAMMENFASSUNG
Zwei einfache Balkenelemente für die statische und dynamische Berechnung von Stahlbetonbauteilen unter Biegung, Schub und Normalkraft werden dargestellt und die zugrundegelegten Annhamen angegeben. Durch den Vergleich von numerischen mit analytischen und experimentellen Resultaten wird die Anwendbarkeit der Modelle aufgezeigt.

1. INTRODUCTION

Theoretical investigations of statically and dynamically loaded structures are based on a variety of diverse mathematical models, which - corresponding to their complexity - allow a more or less accurate idealization of real structural behavior. In order to make a critical examination of these models feasible and to differentiate possible fields of application, essentially two basic model types are distinguished.

On the one hand, local phenomena of structural components are frequently studied with microelements, based on continuum mechanics. The range of possible utilization, however, is narrowly restricted by the often prohibitive computing time and by the excessive storage capacity required. Moreover in many cases this type of model leads to an overestimation of the accuracy of results, because the effects of the basic assumptions on the global behavior are often difficult to estimate.

On the other hand, when using macromodels, the knowledge of the physical phenomena at the level of the structural component is essentially. The simplicity and economy of these models are sometimes offset by severe restrictions on its applicability.

As part of a research project at the Swiss Federal Institute of Technology Zurich on the dynamic behavior of structures in the inelastic range a finite element (FE) computer program (PIFF) has been developed which enables the implementation of different FE-formulations. The application of the program to the analysis of real structures has been the objective from the beginning, so that computational efficiency and physical reliability have been equal criteria in the development of the models. The result of this concept has been the decision, neither to strive for refinements of sophisticated micromodels nor to search for modifications of existing macromodels, but to develop models, which make understandable the inelastic dynamic behavior of structures in their fundamental characteristics.

A first limitation has been adopted in the choice of types of structures: for the present only plane systems are considered, since many structures may be idealized very well by plane frames, trusses and/or shear walls. The development of models therefore has been undertaken for plane structural components, which usually are loaded with moments, normal and shear forces. According to the above specified objective of research, beam finite elements are able to fulfill these requirements.

As theoretical and experimental investigations show, the hysteretic behavior of cyclically deformed reinforced concrete structural components can be very complex. To formulate the relationship between forces and deformations two notions have been widely used:

- Stiffness-Degradation
- Strength-Degradation

Hence, practical requirements for FE-formulations result from the fact that they should idealize stiffness and strength behavior without a full knowledge of the occurring phenomena at the level of structural components. This behavior is mainly influenced by:

- Properties of steel and concrete
- Bond behavior
- Loading combinations
- Loading history

The present elements idealize the interaction between steel and concrete assuming rigid bond, because in many cases bond properties can be neglected and moreover the exact treatment of the problem requires a three-dimensional analysis.

In chapter 3 a simple beam element for bending and normal forces is described, while in chapter 4 a model is presented which includes also shear effects. A few FE-concepts are summarized, as far as they are indispensable in explaining the beam elements.

2. FINITE ELEMENT CONCEPTS

2.1 Fundamentals

To study complex physical problems, the three-dimensional continuum generally is transformed into a discrete system and then solved with numerical methods. In most cases in structural engineering today, this space discretization is performed with the well-known finite element method. Therein, the behavior of a single finite element can be described using the concepts of equilibrium loads and tangential stiffness matrix.

On the element level (subscript e) the equilibrium load vector is given by

$$\{F\}_e = \int_{V_e} [B]^T \{\sigma\}\, dV \qquad (1)$$

where $[B]$ relates the increments of strains $\{\varepsilon\}$ and nodal displacements $\{w\}_e$: $d\{\varepsilon\} = [B]\, d\{w\}_e$. The coefficients B_{ij} are easily derived from the underlying element shape functions. The stress vector $\{\sigma\}$ in cyclic loading depends not only on the strain vector $\{\varepsilon\}$, but also on the entire stress-strain history. It must be mentioned that strains and stresses may also be interpreted as generalized quantities.

The corresponding tangential stiffness matrix can be evaluated by a similar integration (e.g. geometric linear, first order analysis)

$$[K_T]_e = \int_{V_e} [B]^T [D_T][B]\, dV \qquad (2)$$

where $[D_T]$ symbolizes the incremental constitutive law of the material: $d\{\sigma\} = [D_T]\, d\{\varepsilon\}$. If a geometrical nonlinear formulation is required, both initial displacements and stress parts have to be taken into account [1].

2.2 Beam Theory

A special case of the above-sketched discretization is obtained if the three-dimensional displacements of a single element are reduced to shape functions, valid for a line element only. This so-called beam theory will be reviewed shortly. The simplifications of the continuum causes a loss of information, which consequently has to be replaced by a set of appropriate assumptions.

For instance, the commonly used classical beam theory postulates:

- Cross sections maintain their shape
- Cross sections remain plane and perpendicular to the beam axis (hypothesis of Navier-Bernoulli)

These assumptions yield the strains in any point of the element. It is easily shown that only longitudinal strains occur. Hence, no strains perpendicular to the

axis and no shearing deformations are permitted. This implies the violation of the equilibrium conditions within the element and on its boundary and, even more important, allows for no interaction between the shear and the other section forces: the shear force, therefore, is to be perceived as a reaction. Furthermore, directly from the assumption of plane cross sections follows the concept of a rigid bond between steel and concrete. Within the framework of this theory, no other bond law can be specified.

An extension of this classical theory can be obtained by abandoning the assumption cross sections remain perpendicular to the deformed axis. An additional shape function for the angle between the perpendicular and the beam axis leads, in contrast to the above remarks, to shear strains within the element. Using this extension to the classical theory, the interaction between the three section forces can be taken into account in some cases. For reinforced concrete beam elements, however, this approach has to be completed by an additional mode shape, as will be shown in chapter 4.

3. BEAM ELEMENT FOR BENDING AND NORMAL FORCES

Prior to describing the new element, a few notes on customary idealizations will be helpful for the classification of the element and for the subsequent comparisons.

The direct relationship between generalized strains and stresses (e.g. moment-curvature) is usually taken for granted in the derivation of the relatively simple macroelements. Provided that the occurring physical phenomena are well-known and simple enough to formulate, this method of solving engineering problems is advantageous and reasonable. Unfortunately, the inelastic cyclic behavior rarely can be modeled realistically with an elementary stress-strain relationship such as the bilinear law, the Ramberg-Osgood-function or more sophisticated hysteresis laws. In many cases, the properties and the amount of steel and concrete, the level of normal forces (also changing normal force) and the deformation history complicate the structural behavior, so that a generally applicable element formulation is very difficult to realize.

Another often used idealization is the layer-model. In this model the concrete cross section is subdivided into small layers over the height. These individual layers then contribute to the behavior of the element by summation. The steel is treated separately in the same way. This procedure is straightforward and correct within the framework of the classical beam theory, but one can easily imagine, that for practical applications the computational efforts and storage requirements will become prohibitive.

3.1 Model Assumptions

In contrast to the layer-model the proposed element idealizes the concrete contribution to both the equilibrium load vector and the stiffness matrix with only two layers. Obviously, this would be a very crude approximation of the cross section if these layers, here denoted as stringers, were constant in area and position. Thus, the concept of variable stringers has been introduced, observing the classical beam theory. This means that the stringer areas are directly dependent on the position of the neutral axis or, in other words, on the generalized strains of the considered cross section.

The idealizations of the actual stress and stiffness distributions are shown in Fig. 1. The reference points for which the stringer areas (F_t, F_b) and the per-

tinent stresses (σ_t, σ_b) are to be evaluated are assumed to lie in the middle of the stringer areas. Within a stringer the stress distribution is assumed constant, since in general further information is lacking. The same assumptions are made for the stringer stiffnesses (E_t, E_b) and also the lever arms (z_t, z_b) are defined by these reference points. This implies that the concrete strain histories refer to points, varying over the beam height. Fig. 2 shows all strain and one possible appertaining stress distribution, which have to be distinguished.

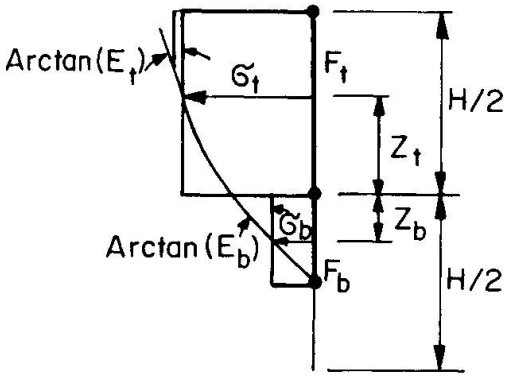

Fig. 1 Idealizations

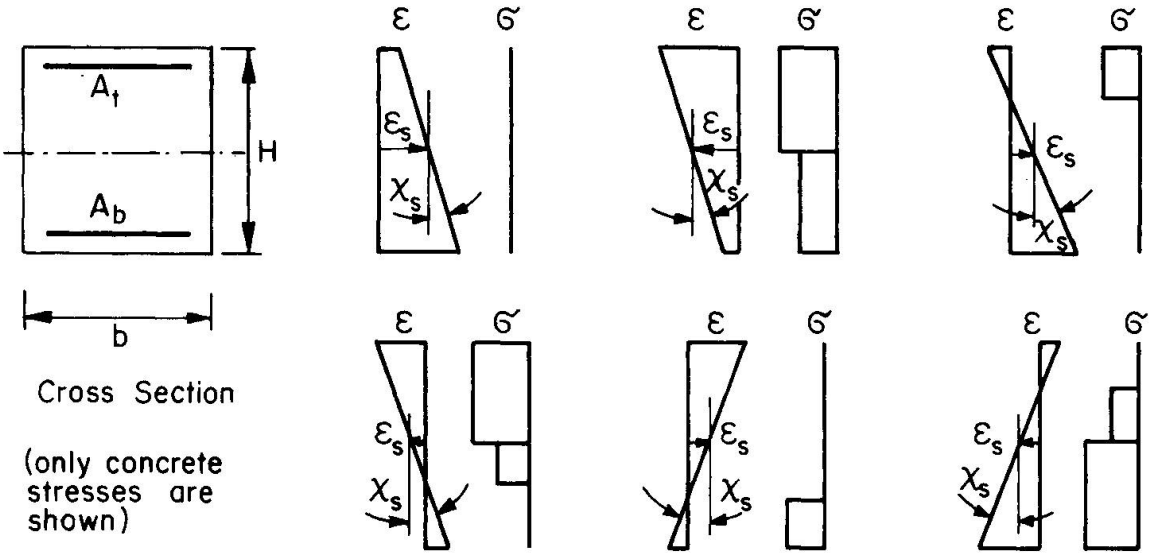

Fig. 2 Strain and Stress Distributions

Mathematically, the previously explained idealizations can be quickly realized. Starting with Eq. 1 for the equilibrium load vector, a numerical integration can be performed, if the generalized section forces $\{\sigma\} = \{N,M\}$ and the kinematical matrix $[B]$ are known. In the discussed element, the matrix $[B]$ has been derived from the commonly-used hermitian polynoms, while the concrete contribution of $\{\sigma\}$ is calculated directly by summing the expressions for the bottom (b) and top (t) stringer. Steel behavior is treated in an analogous manner. In order to keep the mathematical expressions as clear as possible, in this paper these additional terms are not listed.

With the symbols of Fig. 1, it follows:

normal force $$N = \sum_{b}^{t} \sigma F \qquad (3)$$

bending moment $$M = \sum_{b}^{t} \sigma z F \qquad (4)$$

According to the model concept, the three terms σ, z and F are functions of the

generalized strains ε_s and χ_s.

For the evaluation of the tangential stiffness matrix (Eq. 2), in addition to the matrix [B] the knowledge of the constitutive law $[D_T]$ in generalized quantities is required. The coefficients of this matrix are given by the partial derivatives of the section forces with respect to the axial strain ε_s and the curvature χ_s.

$$\frac{\partial N}{\partial \varepsilon_s} = \sum_b^t \left(\frac{\partial \sigma}{\partial \varepsilon_s} F + \sigma \frac{\partial F}{\partial \varepsilon_s}\right) \tag{5}$$

$$\frac{\partial N}{\partial \chi_s} = \sum_b^t \left(\frac{\partial \sigma}{\partial \chi_s} F + \sigma \frac{\partial F}{\partial \chi_s}\right) \tag{6}$$

$$\frac{\partial M}{\partial \varepsilon_s} = \sum_b^t \left(\frac{\partial \sigma}{\partial \varepsilon_s} z F + \sigma \frac{\partial z}{\partial \varepsilon_s} F + \sigma z \frac{\partial F}{\partial \varepsilon_s}\right) \tag{7}$$

$$\frac{\partial M}{\partial \chi_s} = \sum_b^t \left(\frac{\partial \sigma}{\partial \chi_s} z F + \sigma \frac{\partial z}{\partial \chi_s} F + \sigma z \frac{\partial F}{\partial \chi_s}\right) \tag{8}$$

It should be mentioned that the resulting stiffness matrix is no longer symmetric due to the geometrically changing terms $\partial F/\partial \varepsilon_s$, $\partial F/\partial \chi_s$, $\partial z/\partial \varepsilon_s$ and $\partial z/\partial \chi_s$. In order to incorporate this finite element into a customary FE program, it is necessary to neglect the nonsymmetric parts. Nevertheless, for algorithms with equilibrium iterations convergence can be reached with a reasonable tangential stiffness approximation.

3.2 Applications

So far, nothing has been assumed for the steel and concrete properties. In order to estimate the accuracy of the model the behavior of a cross section predicted by this model will be compared with the exact solutions.

First, linear behavior of steel and concrete is considered. The tensile strength of concrete is neglected. Obviously, the normal force N is modeled exactly for all possible strain distributions, while the moment M is only an approximation due to the fact that the lever arm in general is underestimated. In Fig. 3 the relative error of the moment is shown as a function of the neutral axis. As can be seen, for $\xi \leq 0.25$ the relative error is very small, while for $\xi \geq 0.5$ the relative error is up to 25%. The presence of reinforcement improves the solution.

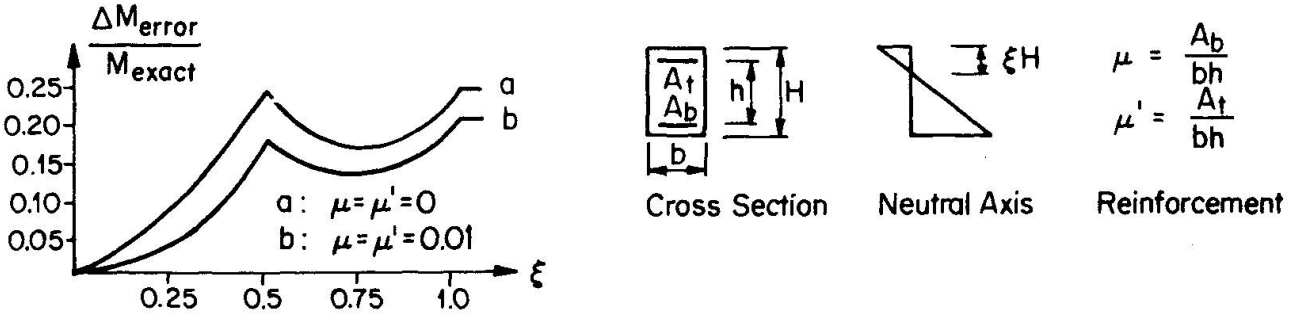

Fig. 3 Accuracy for the Stringer Model (linear elastic material)

As second example rigid-plastic material behavior is taken, neglecting again the tensile strength of the concrete. In this case only a prediction of strength is obtained. The idealization gives the exact solution since not only the stress distribution, but also the lever arm is correct. Fig. 4 shows the interaction curves for two different parameters.

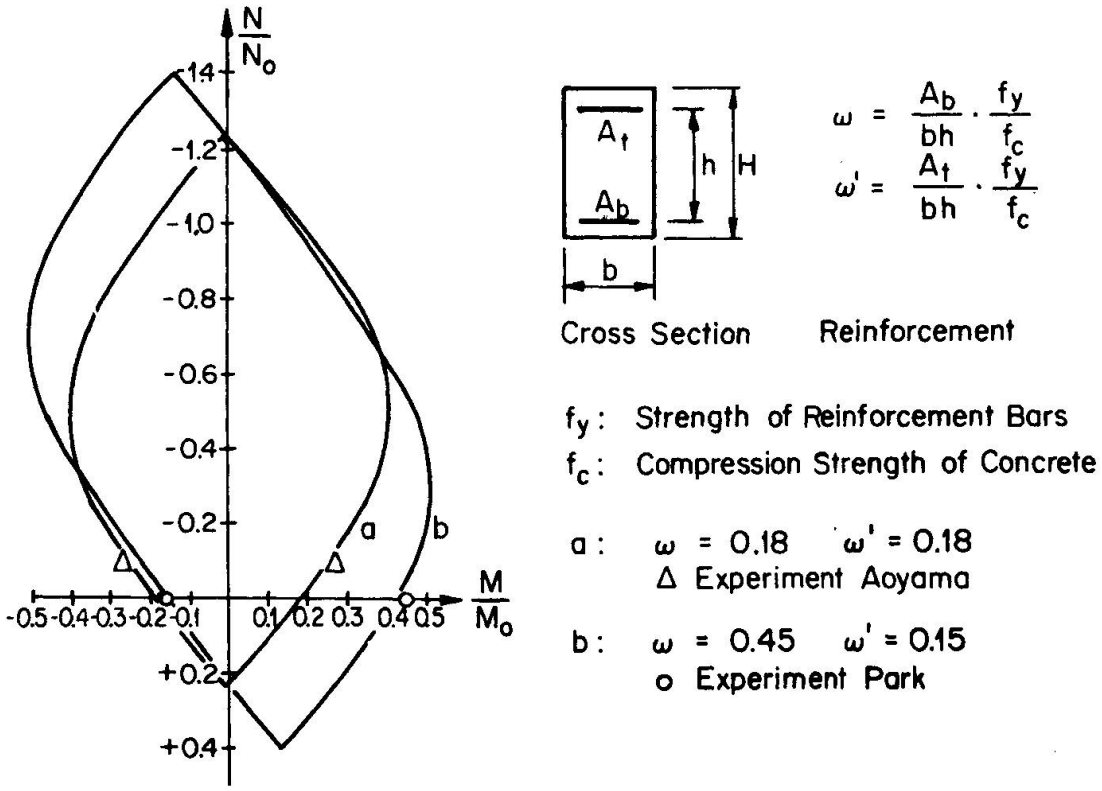

Fig. 4 Interaction Curves (rigid plastic material)

The preceding examples have been used to qualitatively show the accuracy of the proposed model. In the following, more realistic material behavior will be considered.

The steel properties are modeled with the well-known Ramberg-Osgood-function, adopting the procedures and the empirical data proposed by Park [2].

For cyclic one-dimensional concrete behavior, three different concrete models are implemented in the FE program and may be used alternatively, depending on the problem. Typical cyclic behavior of the three models is sketched in Fig. 5.

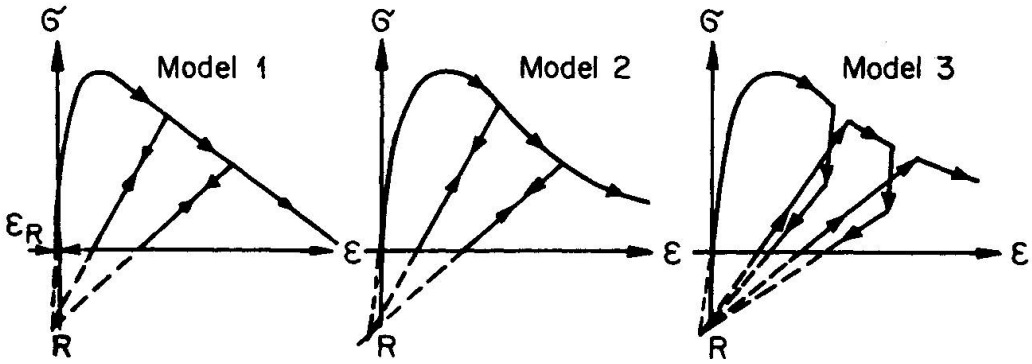

Fig. 5 Typical Stress-Strain-Relationship of Concrete Models

Models 1 and 2 differ only in the descending branch of the stress-strain relationship. In both models, the unloading path is directed towards an appropriately selected point R and therefore the unloading stiffness becomes dependent on the maximum of the compression strain.

Model 3 additionally allows for plastic strain increments by applying constant stress amplitudes. By deforming the concrete with constant strain amplitudes a reduction of the stress amplitude will result.

Following are several comparisons between experimental results and theoretical values using the above mentioned stress-strain relationships for steel and concrete.

First, a few cycles from experiments performed in Zurich [3] are compared with the FE calculations. The statical system and the loading are shown together with the pertinent FE idealization in Fig. 6. As can be seen, the FE solution is always too stiff. The main reasons for this observation is found in the very rough FE mesh. Since a displacement based model is used, the calculated response of the beam must be expected to be too stiff. Comparing the same results for the moment-curvature relationship, the agreement between experiment and the FE calculation is more satisfying.

The next example illustrates the influence of a constant compression force on a symmetrically reinforced concrete cross section, loaded with bending moments according to a given curvature history [2].

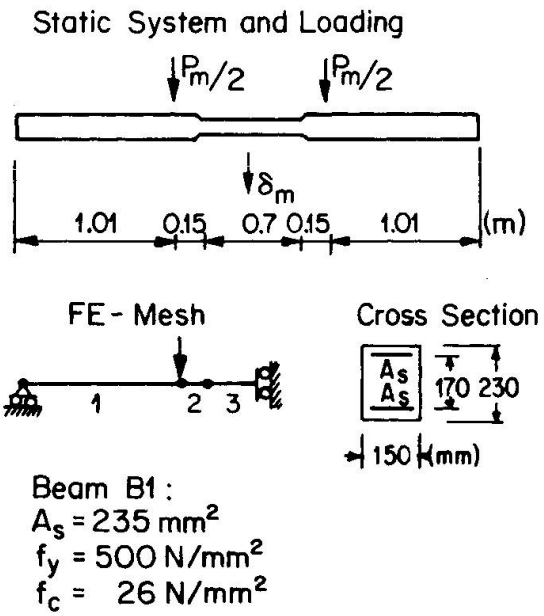

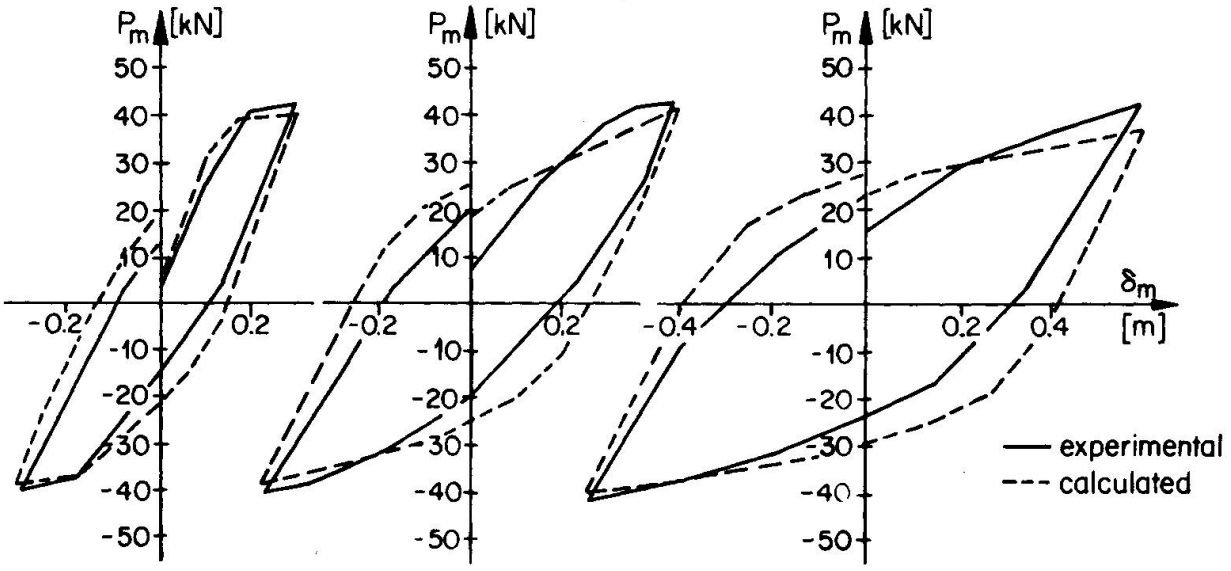

Fig. 6 Comparison I between FE-Calculation and Experiment [3]

Again the agreement between the experimental and computed values is good (Fig.7). The yielding of the reinforcing bars in compression and the subsequent closing of the cracks - the cause of the pinched form of the hysteresis - can be modeled

quite well with the proposed model. A complementary comparison can be performed by plotting the positive and negative extreme moments M_{ult} into the corresponding nondimensional interaction curve (Fig.4).

The last example shows the hysteretic behavior (moment-curvature) of a reinforced concrete cross section with different top and bottom reinforcement [2]. The imposed curvature history is typical for earthquake-loaded structures. Once more the strength in both directions is simulated very well, while the stiffness shows more deviation. In Fig. 4 the positive and the negative extreme moments M_{ult} are plotted on the interaction curve.

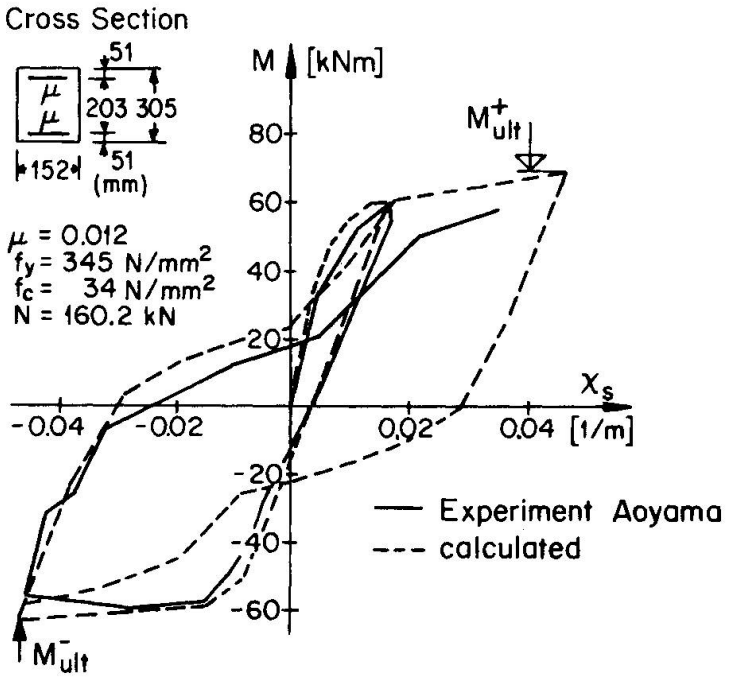

Fig. 7 Comparison II between FE-Calcultation and Experiment [2]

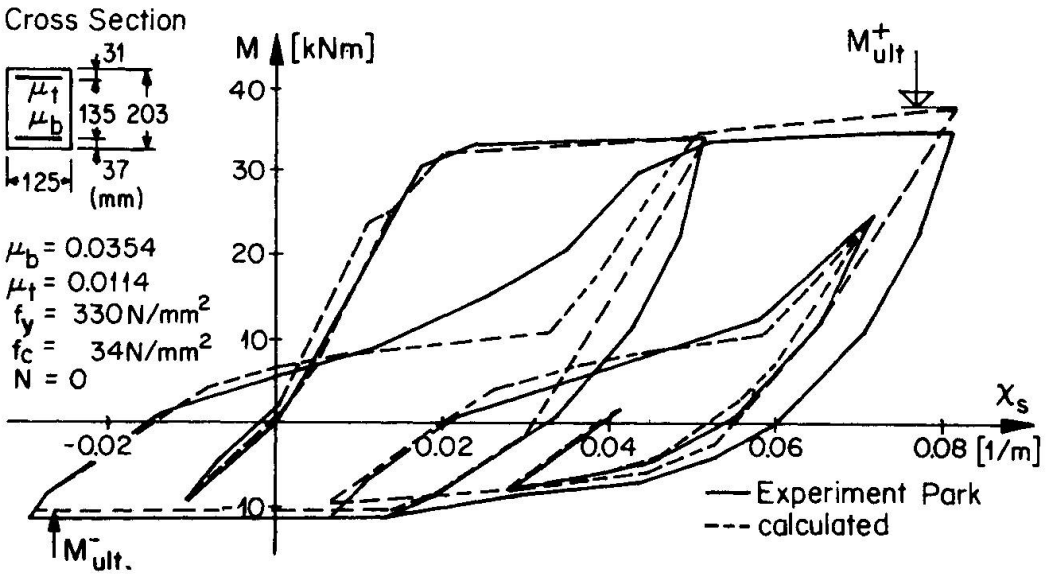

Fig. 8 Comparison III between FE-Calculation and Experiment [2]

In order to show the field of application of the proposed element, a brief estimation is carried out. As has been demonstrated in Fig. 3 accurate solutions may be expected if the compression portion of the cross section is relatively small. Since in cyclic loading the yielding of the reinforcement causes an opening of the cracks, the behavior of the reinforcement plays a major role in most cases. Only for high normal forces larger parts of the concrete cross section will contribute considerably to the section forces, and thus influence the behavior significantly. Hence, the limited reliability for high normal forces must be kept in mind. However, as can be seen in Fig. 1, the more the concrete is strained, the better the stress idealization coincides with the actual stress distribution. Hence, improved accuracy will result for such cases.

4. BEAM ELEMENT FOR BENDING, SHEAR AND NORMAL FORCE

4.1 FE Models for Shear Problems

If in addition to bending and normal forces, shear forces must also be taken into account, the idealization of structural members with two- or three-dimensional FE is commonly accepted. This means that the concrete is modeled with multidimensional isoparametric FE, whereas a uniaxial discretization for the reinforcing bars is chosen. The simulation of bond effects can be performed with additional spring elements.

This procedure is conceptually straightforward but, as mentioned earlier, for actual structures becomes impracticable. Furthermore, from an engineering point of view, the enormous flow of local stress-strain histories is not very meaningful and complicates control and judgement of the results.

In the following, attention will be focused on structural members which are significantly influenced by shear forces, although geometrically they are idealized as beam elements. The proposed generalized new beam element seems to be of interest since - compared to multidimensional FE - the computational efficiency, the facility of the specified input and the critical estimation of results are improved. The development starts from the extended beam theory including shear deformations. For both steel and reinforced concrete members this theory will be generalized in this paper. The cross sectional shape is restricted to rectangular, T- and I-sections. Flange bending is neglected since the flanges and the longitudinal reinforcing bars are idealized as one-dimensional stringers.

4.2 Assumed Shape Functions

In order to allow for shear displacements it is convenient to formulate the shape functions in natural modes, as shown in Fig. 9.

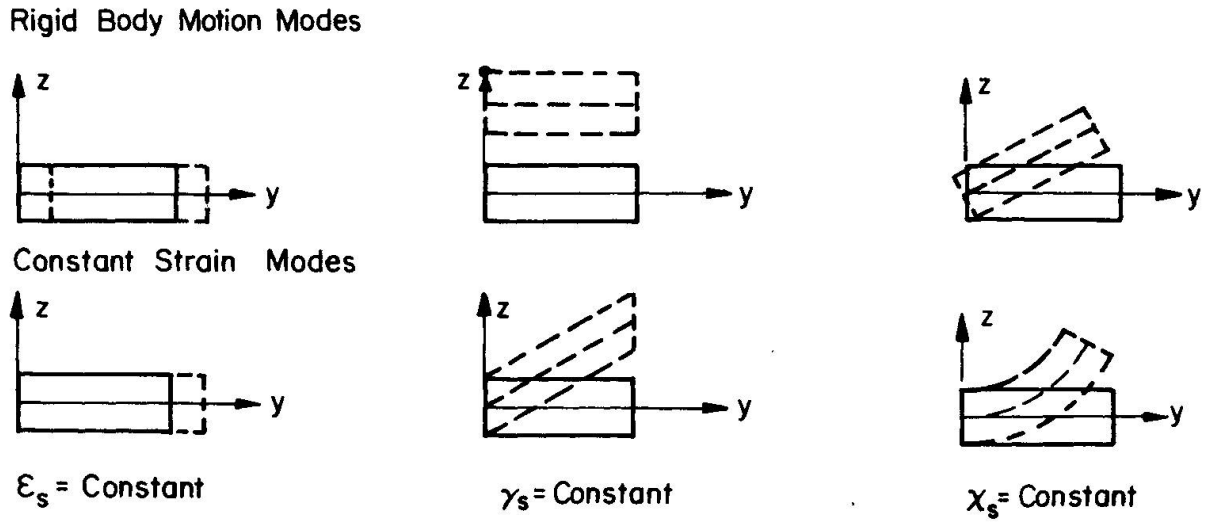

Fig. 9 Modal Shapes

The given modes correspond to constant section forces over the element length, which permits the use of a single integration point in the longitudinal direction for the evaluation of the equilibrium loads and the tangential stiffness matrix. The simultaneous assumption of constant shear force and bending moment

are inconsistent, but for displacement FE models this inconsistency is not important. Therefore a stepwise approximation results in the actual moment distribution.

Blaauwendraad et al. [4] proposed a model, which shows similarities to the present one. In the following sections, some differences will be discussed.

4.3 Nodal Displacements, Strains and Stress-Strain Properties

As noted earlier, the incremental relationship between the generalized element strains and the nodal displacements is given by

$$\begin{Bmatrix} d\varepsilon_s \\ d\gamma_s \\ d\chi_s \end{Bmatrix} = [B]\, d\{w\}_s \tag{9}$$

By applying the concept of the extended beam theory, the uniaxial longitudinal strains ε_{st} in the stringers as well as the longitudinal strain ε_y and the shearing strain γ_{yz} over the cross section height are found.

For the web section, an isotropic two-dimensional incremental material law is adopted

$$\begin{Bmatrix} d\sigma_y \\ d\sigma_z \\ d\tau_{yz} \end{Bmatrix} = [D_T] \begin{Bmatrix} d\varepsilon_y \\ d\varepsilon_z \\ d\gamma_{yz} \end{Bmatrix} \tag{10}$$

So far, no information on the actual vertical strain ε_z can be gathered from the chosen mode shape. Two extreme cases are conceivable:

$\sigma_z = 0$ i.e. completely unrestrained boundary condition in the z-direction

$\varepsilon_z = 0$ i.e. rigid boundary condition in the z-direction

To judge the reliability of these assumptions, different material properties will be discussed.

Steel Members

The hypothesis of unrestrained vertical boundary condition ($\sigma_z = 0$) is usually reasonable for steel beam elements; computed and experimental results are well in agreement (see chapter 4.5). Steel generally is idealized with homogeneous and isotropic material behavior. For the element under consideration the well-known Von Mises yield criterion with a kinematic hardening rule has been implemented into the program.

Reinforced Concrete Members

In the case of elements composed of concrete and steel, the boundary conditions $\sigma_z = 0$ as well as $\varepsilon_z = 0$ do not reflect the actual behavior of reinforced concrete members at all. Rather, the constraining influence of the stirrups on the concrete plays a major role in the mechanism of shear transfer; that is, the stirrups act as an elastic-plastic support for the concrete web. In the proposed model the influence of the stirrups is "smeared" over the element length.

In order to show the consequences of typical multiaxial yield conditions - sensitive to the hydrostatic pressure - on the behavior of reinforced concrete members, the Drucker-Prager yield criterion (Fig. 10) is used to idealize the

strength behavior of concrete. It is a rather crude approximation for the actual concrete behavior. For problems where concrete fails predominantly in multiaxial compression, a refined material formulation with at least three parameters must be used. Otherwise, the strength is strongly overestimated. Furthermore, for cyclic behavior an even more sophisticated formulation has to be adopted. However, the chosen yield criterion will suffice to explain the element.

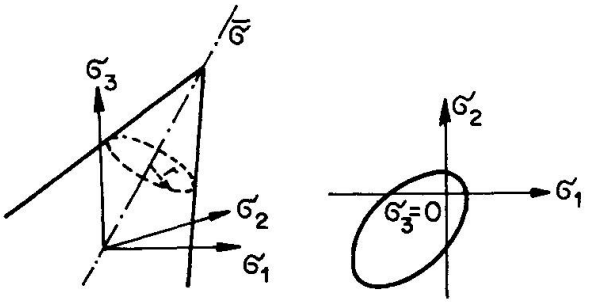

Fig. 10 Drucker-Prager (extended v. Mises) Yield Criterion

4.4 Additional Degree of Freedom

In order to complete the missing information about the strain component ε_z additional mode shapes are considered. This can be realized in two different manners, by introducing either internal or external degrees of freedom.

Internal, Element-Related Degree of Freedom

The additional mode shape is shown in Fig. 11. It corresponds to a constant strain state ε_z in the entire element. As can be seen the element is kinematically noncompatible, as at the element boundaries displacement continuity may be violated.

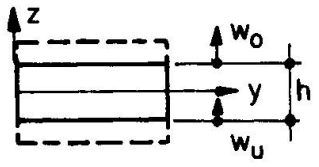

$$w_7 = w_0 - w_u \qquad \varepsilon_z = \frac{w_7}{h}$$

Fig. 11 Additional Internal Mode

Using the notions of Fig. 11 the incremental relationship between the generalized strains and the nodal displacements can be written

$$\begin{Bmatrix} d\varepsilon_s \\ d\gamma_s \\ d\chi_s \\ d\varepsilon_z \end{Bmatrix} = \begin{bmatrix} [B] & \cdot \\ \cdot & \frac{1}{h} \end{bmatrix} \begin{Bmatrix} d\{w\}_e \\ dw_7 \end{Bmatrix} \tag{11}$$

The contributions to the equilibrium load vector and to the stiffness matrix can be taken into account by adding the parts of the concrete web and the "smeared" stirrups.

First, the actual stiffness matrix (6x6) is derived from the original element stiffness matrix (7x7) by a standard condensation procedure. This derivation results in the relationship between the 6 external and the internal parameters as well. In order to achieve global equilibrium, element internal iterations in the added degree of freedom (dw_7) are performed first and then the equilibrium loads are evaluated by numerical integration. This redistribution of the unbalanced forces has to be performed for each time or load step so that accuracy and convergence is guaranteed. The setting up of the tolerance parameters requires good engineering judgement and experience. Otherwise this iteration procedure may become too time-consuming for practical analysis.

External, Global Degree of Freedom

The strain state ε_z alternatively can be realized by adding a global nodal parameter to the three commonly-used joint parameters.

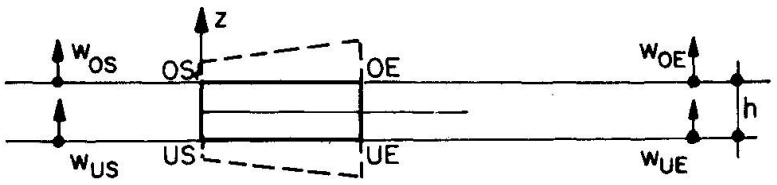

Fig. 12 Additional Internal Mode

Keeping one integration point in the middle of the element, the additional degrees of freedom correspond to a constant strain state $\varepsilon_z = 1/2h\ (w_7+w_8)$. This formulation introduces one kinematical mode at element level; in order to prevent the resulting instabilities in the global system, adequate boundary conditions must be specified.

This procedure (not yet implemented) seems to be more efficient than the one previously explained since unbalanced load components can be redistributed simultaneously. On the other hand, a larger number of degrees of freedom is involved and difficulties may arise in defining boundary conditions (e.g. joints with more than two incidences). Furthermore, flexible problem-dependent convergence criteria will become complicated.

The approach presented by Blaauwendraad et al. [4] shows some similarities with the present model. However, in contrast to the proposed element, layer techniques, linear generalized strain states and a different material formulation are used.

4.5 Numerical Investigation

Simply-supported Steel Beam

Experimental results of simply-supported steel beams have been reported by K. Brandt et al. [5]. The plastic irreversible deformation pattern of one of these beams (Fig. 13) is characterized by the shear yielding of the web. For analysis, one-half of the beam was idealized with three elements. Predicted and experimental responses are shown in Fig. 14.

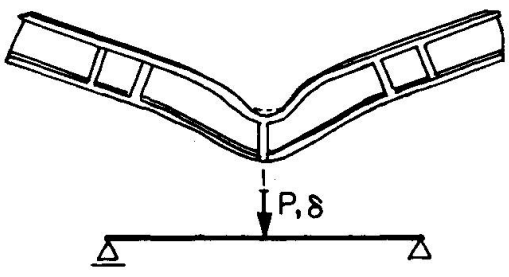

Fig. 13 HEM-160, Beam A3 [5]
$f_y = 360\ N/mm^2$
$f_u = 540\ N/mm^2$

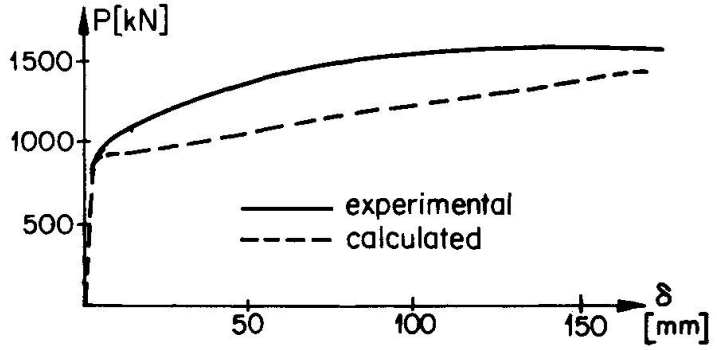

Fig. 14 Load-Displacement Diagrams

Steel Frame

The response of a plane steel frame (Fig. 15) was expected to be governed by shear and large-displacement effects. Hence, for a first idealization 25 two-dimensional isoparametric elements for the webs and 100 truss elements for the flanges were

used. Geometrical and material nonlinearities (von Mises yield criterion, kinematical hardening) were taken into account. The analysis was stopped prematurely since the load increment required for convergence had become extremely small and the costs unreasonable high.

Using the above-explained shear beam element for the same problem, the calculation was performed successfully with a computing time of about 10% of that required for the two-dimensional isoparametric element analysis.

A comparison calculation was carried out with a simple moment-curvature element. Since it accounts for bending effects only, the strength of the beam is strongly overestimated as can be seen in Fig. 16.

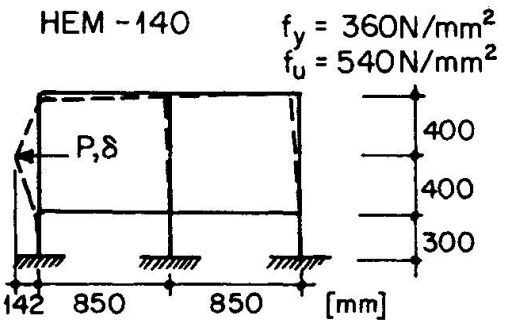

Fig. 15 Frame Displacements at Failure

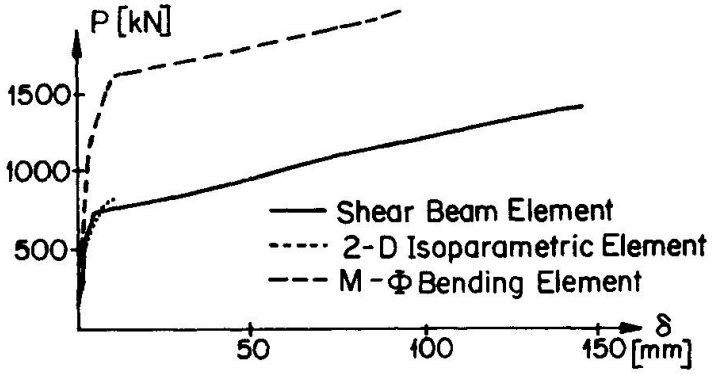

Fig. 16 Load-Displacement Diagrams

Reinforced Concrete Beam Subjected to Pure Shear

The web of a reinforced concrete beam can be idealized as a shear wall subjected to pure shear. To describe this behavior analytically truss models with inclined compression struts (Fig. 17) have been applied widely [6] and constitute the theoretical background of the Directive 34 of the Swiss Code 162.

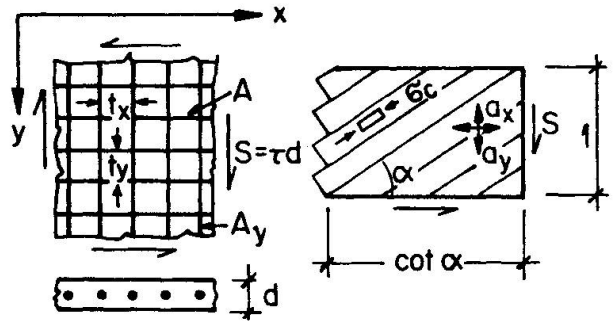

$$a_x = \frac{A_x}{t_y} \qquad p_x = a_x f_{sx}$$

$$a_y = \frac{A_y}{t_x} \qquad p_y = a_y f_{sy}$$

f_{sx}, f_{sy} : Yield Stresses

Fig. 17 Shear Web Model [6]

In order to compare the FE-idealization with the analytical model, the expected inclination of the compression struts are plotted in Fig. 18. Five different reinforcement ratios p_y/p_x are considered. In the present example the amount of reinforcement was chosen small enough, so that failure was reached after yielding of both longitudinal and vertical reinforcement.

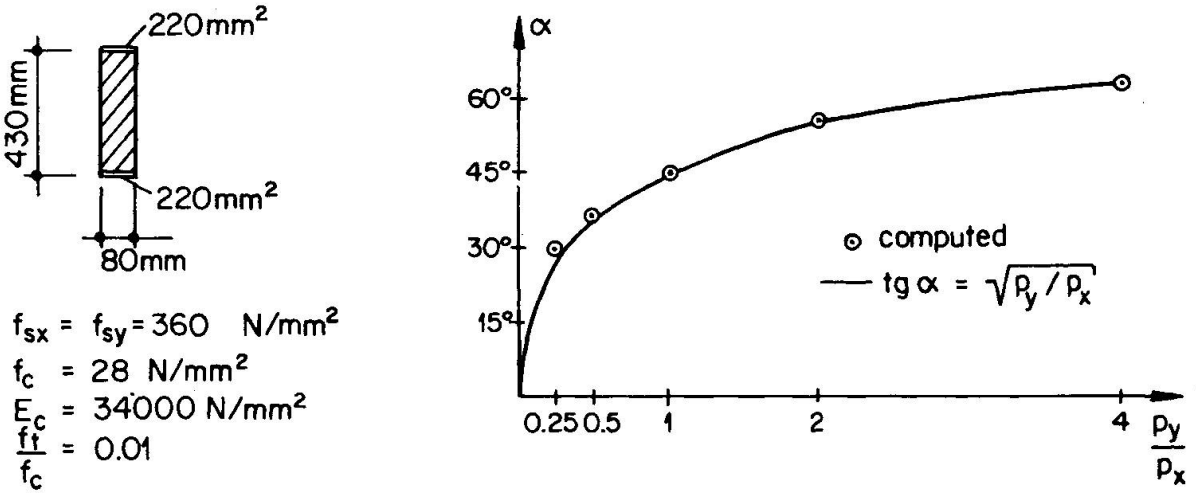

Fig. 18 Analytical and Computed Values of α

A comparison of computed and tested response is presented in Fig. 19. The experimental results have been gathered from the measurements on a box girder subjected to pure torsion [7]. The investigated shear web is shown in Fig.18 (Beam T2: shear reinforcement 1000 mm²/m')

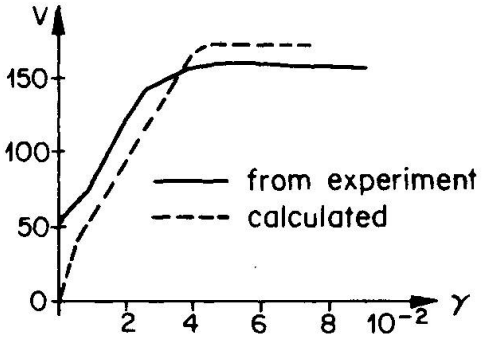

Fig. 19 Shear Force - Shear Strain

Reinforced Concrete Beam Subjected to Bending and Shear

With the above mentioned truss model, bending moment (M) - shear force (V) interaction curves for ultimate strength can be derived [6]. In Fig. 20 a M-V-interaction curve is plotted. The analogous computer analysis has been performed on a single element. In order to obtain some points of the interaction curve the ratio between the applied shear force and resulting bending moment has been varied.

The actual beam cross section is shown in Fig. 18 with a shear reinforcement of 1000 mm²/m' and in accordance with [6] the stringers were assumed very stiff in compression.

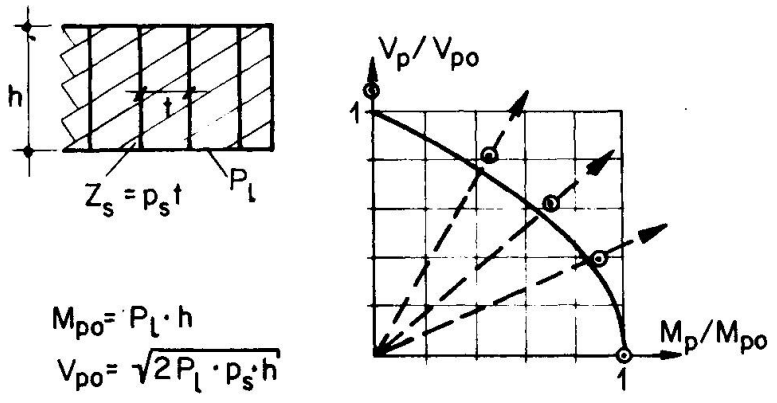

Fig. 20 Bending Moment - Shear Force Interaction Diagram

Considering that numerical computation was performed with $f_t = 0.01\ f_c$ while zero tensile strength is assumed in [6], acceptable agreement is found.

If the bending strength of the web is taken into account for cross sections such as rectangular ones additional shear strength due to the bending compression zone can be expected and was also observed in a numerical investigation. However, the presented - displacement based - FE model fulfills in this case equilibrium within a single element only in a global sense. A trend to overestimate the strength is therefore inherent. Additional research work is needed for definitive conclusions.

A comparison of calculated and measured bending and shear response will be illustrated with a last example. A serie of two span reinforced concrete beams has been tested and reported by Leonhardt et al. [8]. The behavior of beam HH5 was strongly governed by shear effects and the ductile failure of the beam was reached after yielding of bending and shear reinforcement.

In Fig. 22 the computed load-displacement diagram is compared with the experimental curve and in Fig. 21 both the calculated and measured displacement shapes at a load level of 140 kN are plotted. The agreement between experiment and theory is satisfying.

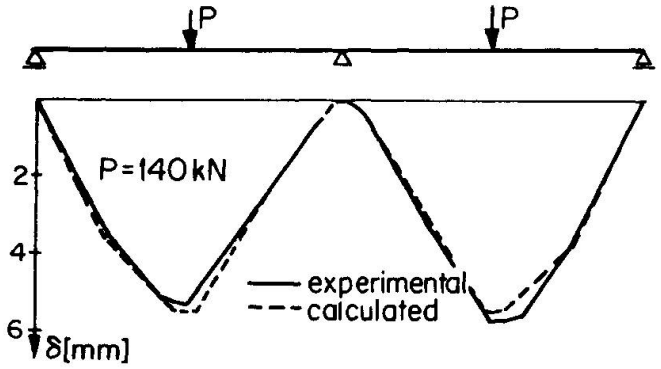

Fig. 21 Displacements of Beam HH5 [8]

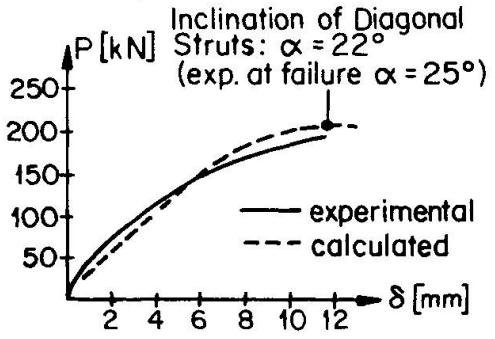

Fig. 22 Load-Displacement Diagram

Summarizing the previous remarks the discussed element models seem to describe adequately the nonlinear behavior of steel and reinforced concrete beams under combined bending and shear. Applicability is limited by the assumed simple constitutive laws for concrete and steel and by possible stiffening effects due to local equilibrium violations as explained above. While the first restriction is not inherent to the model itself, further studies are under way in order to improve equilibrium fulfillment within the element.

REFERENCES

[1] O.C. Zienkiewicz, "The Finite Element Method in Engineering Science", McGraw Hill, 1971
[2] R. Park, T. Paulay, "Reinforced Concrete Structures", John Wiley & Sons, Inc., 1975
[3] M. Rossi, B. Thürlimann, "Das Verhalten von Stahlbeton-Balken bei wiederholter Belastung", Institut für Baustatik und Konstruktion, ETH Zürich, Bericht Nr. 7503-1, Mai 1981
[4] J. Blaauwendraad,S.F.C.H. Leijten, J.G.M. van Mier, "Comparison of Plastic Prediction with STANIL/1 Analysis", IABSE, Vol. 29, Copenhagen 1979
[5] K. Brandt, S. Klee, "Traglastversuche an gewalzten Breitflanschprofilträgern", Der Stahlbau, 7/1979
[6] B. Thürlimann, "Plastic Analysis of Reinforced Concrete Beams", IABSE, Vol. 28, Copenhagen 1979
[7] P. Lampert, B. Thürlimann, "Torsionsversuche an Stahlbetonbalken", Institut für Baustatik und Konstruktion, ETH Zürich, Bericht Nr. 6506-2, Juni 1968
[8] F. Leonhardt, R. Walther, W. Dilger, "Schubversuche an Durchlaufträgern", DAfSt, Heft 163, Berlin 1964